INFECTION AND IMMUNITY, Aug. 2005, p. 4512–4521 Vol. 73, No. 8
0019-9567/05/$08.00+0 doi:10.1128/IAI.73.8.4512–4521.2005
Copyright © 2005, American Society for Microbiology. All Rights Reserved.

# A Toll-Like Receptor 2-Responsive Lipid Effector Pathway Protects Mammals against Skin Infections with Gram-Positive Bacteria

Philippe Georgel,[1] Karine Crozat,[1] Xavier Lauth,[2] Evgenia Makrantonaki,[3] Holger Seltmann,[3] Sosathya Sovath,[1] Kasper Hoebe,[1] Xin Du,[1] Sophie Rutschmann,[1] Zhengfan Jiang,[1] Timothy Bigby,[1] Victor Nizet,[2] Christos C. Zouboulis,[3] and Bruce Beutler[1]*

*Department of Immunology, The Scripps Research Institute, 10550 N. Torrey Pines Road, La Jolla, California 92037[1]; Department of Pediatrics, University of California, San Diego, La Jolla, California 92093[2]; and Department of Dermatology, Charité University Medicine Berlin, Fabeckstrasse 60-62, 14195 Berlin, Germany[3]*

Received 26 January 2005/Returned for modification 1 March 2005/Accepted 10 March 2005

***flake* (*flk*), an *N*-ethyl-*N*-nitrosourea-induced recessive germ line mutation of C57BL/6 mice, impairs the clearance of skin infections by *Streptococcus pyogenes* and *Staphylococcus aureus*, gram-positive pathogens that elicit innate immune responses by activating Toll-like receptor 2 (TLR2) (K. Takeda and S. Akira, Cell. Microbiol. 5:143–153, 2003). Positional cloning and sequencing revealed that *flk* is a novel allele of the stearoyl coenzyme A desaturase 1 gene (*Scd1*). *flake* homozygotes show reduced sebum production and are unable to synthesize the monounsaturated fatty acids (MUFA) palmitoleate ($C_{16:1}$) and oleate ($C_{18:1}$), both of which are bactericidal against gram-positive (but not gram-negative) organisms in vitro. However, intradermal MUFA administration to *S. aureus*-infected mice partially rescues the *flake* phenotype, which indicates that an additional component of the sebum may be required to improve bacterial clearance. In normal mice, transcription of *Scd1*—a gene with numerous NF-κB elements in its promoter—is strongly and specifically induced by TLR2 signaling. Similarly, the *SCD1* gene is induced by TLR2 signaling in a human sebocyte cell line. These observations reveal the existence of a regulated, lipid-based antimicrobial effector pathway in mammals and suggest new approaches to the treatment or prevention of infections with gram-positive bacteria.**

Surface epithelia constitute the first line of defense against pathogens. This defense depends both on barrier function and on specific microbicidal effector molecules. For example, the mammalian skin affords physical protection partly because it is composed of tightly associated cells covered by a highly cross-linked layer of keratin and is normally impermeable to bacteria. In humans, several genetic diseases, such as mucoepithelial dysplasia or epidemolysis bullosa, which affect the cutaneous epithelial structure at different levels (23, 26), are associated with greatly increased susceptibility to infection. But the skin displays microbicidal activity even when its physical integrity is breached. It contains an arsenal of bioactive molecules, among which antimicrobial peptides (AMPs) such as defensins and cathelicidins are of critical importance to host defense against microbial invasion (reviewed in references 27 and 28).

While AMPs are the best-studied cutaneous defense molecules, other protection systems may also exist. In this regard, several lipids extracted from human skin, among which free fatty acids have been shown to be the most potent molecules, possess antistaphylococcal activity (12). In addition, monounsaturated fatty acids (MUFA) are also produced by the sebaceous glands, and some MUFA are known to be microbicidal (24). However, their contribution to antimicrobial defense has never been established in vivo, nor is their biosynthesis known to be subject to regulation by microbial stimuli. In the present report, a novel innate immunodeficiency phenotype, characterized by a reduced ability to clear an experimental skin infection with gram-positive bacteria in mice, has been traced to a mutation affecting the structure of an enzyme essential for MUFA synthesis.

* Corresponding author. Mailing address: Department of Immunology, The Scripps Research Institute, 10550 N. Torrey Pines Road, La Jolla, CA 92037. Phone: (858) 784-8610. Fax: (858) 784-8444. E-mail: bruce@scripps.edu.

## MATERIALS AND METHODS

**Mice.** Germ line mutagenesis using *N*-ethyl-*N*-nitrosourea (ENU) has been described in reference 7. Animals were maintained under pathogen-free conditions in the animal care facility of the Immunology Department of The Scripps Research Institute. All mice used in the experiments were 8 to 12 weeks old. Handling of mice and experimental procedures were conducted in accordance with institutional guidelines for animal care and use.

**Bacteria.** *Staphylococcus aureus* Xen8.1 (parental strain 8325-4), *Streptococcus pyogenes* Xen20 (derived from serotype M49, strain 591), and *Escherichia coli* Xen14 (derived from EPEC WS2572) were obtained from Xenogen (Cranbury, NJ).

**Cell culture.** SZ95 sebocytes were maintained in HSG-Med (Sebomed, Berlin, Germany) supplemented with 10% heat-inactivated fetal calf serum, 5 ng/ml human epidermal growth factor, 1 mM $CaCl_2$, $10^{-5}$ M palmitic acid, and 50 μg/ml gentamicin for 2, 4, 8, and 18 h with or without 50 ng/ml macrophage-activating lipopeptide 2 (MALP-2) or 100 ng/ml lipopolysaccharide (LPS), and the supernatants were collected for interleukin-6 (IL-6) and IL-8 evaluation by enzyme-linked immunosorbent assay. RNA was isolated from the 4- and 18-hour samples by the RNeasy Midi kit (QIAGEN, Hilden, Germany) and purified by the RNase-Free DNase set (QIAGEN) for reverse transcription-PCR (RT-PCR).

**Reagents.** Palmitoleic and oleic acids were purchased from Sigma. *Salmonella enterica* serovar Minnesota Re595 LPS was obtained from Alexis (Carlsbad, CA) and MALP-2 from EMC microcollections GmbH (Tübingen, Germany).

**Skin infection.** Bacterial cultures in exponential-growth phase were centrifuged, and the pellet was resuspended in 10 volumes of phosphate-buffered saline containing 10 mg/ml of inert Cytodex beads (Sigma) used as a carrier. Approximately $5 \times 10^5$ CFU of luminescent bacteria in 100 μl was injected subcutaneously into the backs of anesthetized animals. Hairs were removed by chemical depilation prior to inoculation. Luminescence was monitored daily with

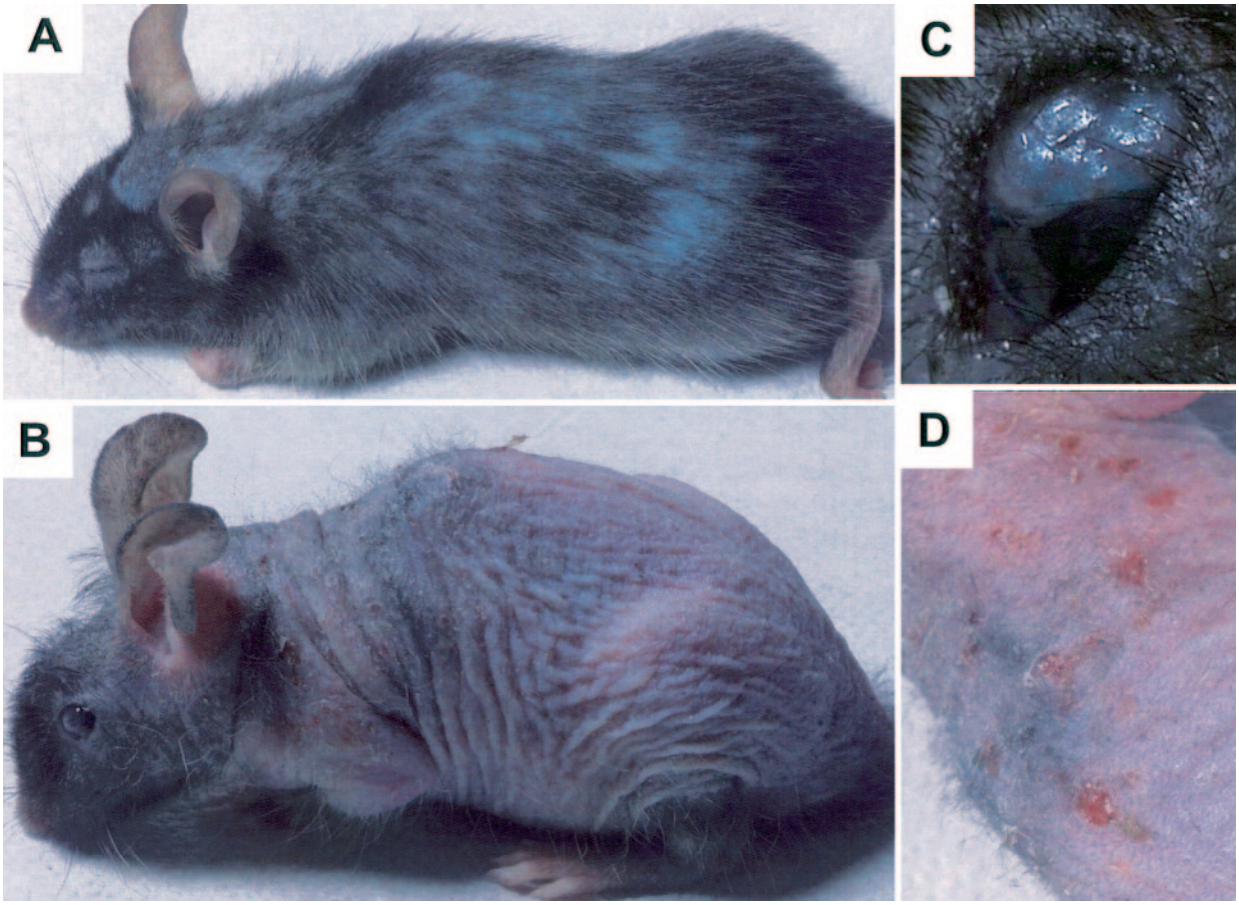


FIG. 1. Visible phenotypes observed in *flake* mutant mice. (A) Six-week-old mouse; (B) 8-month-old mouse; (C) eye infection in an 8-month-old mouse. (D) Magnification of the mouse photograph in panel B highlights severe dermatitis.

a charge-coupled device camera (5-min exposure of animals), and quantification was done with the IVIS program from Xenogen.

**TLC.** Total lipids extracted from skin biopsy specimens by chloroform-methanol were separated by silica gel thin-layer chromatography (TLC). Hexane-diethyl ether-acetic acid (70:30:1) was used as the developing solvent, and lipids were visualized under a UV lamp after being sprayed with a primuline solution (5 mg in 100 ml acetone-water [80/20]).

**Semiquantitative RT-PCR.** Wild-type and *Tlr2*$^{-/-}$ mutant mice were depilated and infected by subcutaneous injection of *S. aureus* or *E. coli* ($5 \times 10^5$ PFU). After 24 h, the skin of the infected area was dissected and total RNA was extracted by the Trizol (Gibco) method. One microgram of RNA was used to synthesize oligo(dT)-primed cDNA (Retroscript; Ambion), which then served as a template in PCRs using primers specific for *Scd1* (3′-CTCTATGGATATCG CCCCTACGACAAGAACATTC-5′ in exon 5 and 3′-GAAGCTAGGAACAA GGAGGGATGTATTCAGGAGG-5′ in exon 6, which allow for a distinction between genomic and cDNA amplification) or β-*actin* genes. Portions (4 μl) of the PCR products were loaded onto agarose gels. Isolation of peritoneal macrophages and stimulation have been described elsewhere (7). *hSCD1* and *hFADS2* expression in SZ95 sebocytes was measured by semiquantitative RT-PCR using the following oligonucleotides: hSCD1f (5′-TTCAGAAACACATG CTGATCCTCATAATTCCC-3′), hSCD1r (5′-ATTAAGCACCACAGCATAT CGCAAGAAAGTGG-3′), hFADS2f (5′-ACTTTGGCAATGGCTGGATTCC TACCCTC-3′), and hFADS2r (5′-ACATCGGGATCCTTGTGGAAGATGTT AGG-3′). Glyceraldehyde-3-phosphate dehydrogenase (GAPDH) expression was used as a control.

## RESULTS

*flake*: a visible phenovariant with associated immunodeficiency. In an effort to identify genes required for normal immune function, we have screened a total of 20,792 $F_1$ and 33,202 $F_3$ animals with ENU-induced germ line mutations for visible and immunologic phenotypes. Among these, a recessive mutation dubbed "*flake*" (*flk*) was found to cause progressive alopecia and chronic exfoliative dermatitis. These features appeared at weaning age and were more pronounced in older animals (Fig. 1). Visible disruption of epidermal integrity and sporadic spontaneous skin infections requiring antibiotic therapy prompted us to examine the integrity of the innate immune function in these mice.

**Persistent *Streptococcus pyogenes* and *Staphylococcus aureus* skin infections in *flk*/*flk* mutant mice.** The gram-positive cocci *S. pyogenes* and *S. aureus* are the leading agents of human impetigo, cellulitis, and wound infection (5, 6). Experimental full-thickness skin infection in the murine model can be reliably established by immediate subcutaneous injection with a fine-gauge needle (2, 14), overcoming the requirement for traumatic injury and the poor infectivity and reproducibility associated with epicutaneous inoculation (8).

We utilized luminescently tagged strains of *Streptococcus pyogenes*, *Staphylococcus aureus*, and *Escherichia coli*, each of which constitutively expressed a bacterial *lux* operon derived from *Photorhabdus luminescens* (9). The progress of each infection was monitored by external luminometry over a period of 16 days in anesthetized mice. As shown in Fig. 2A, normal

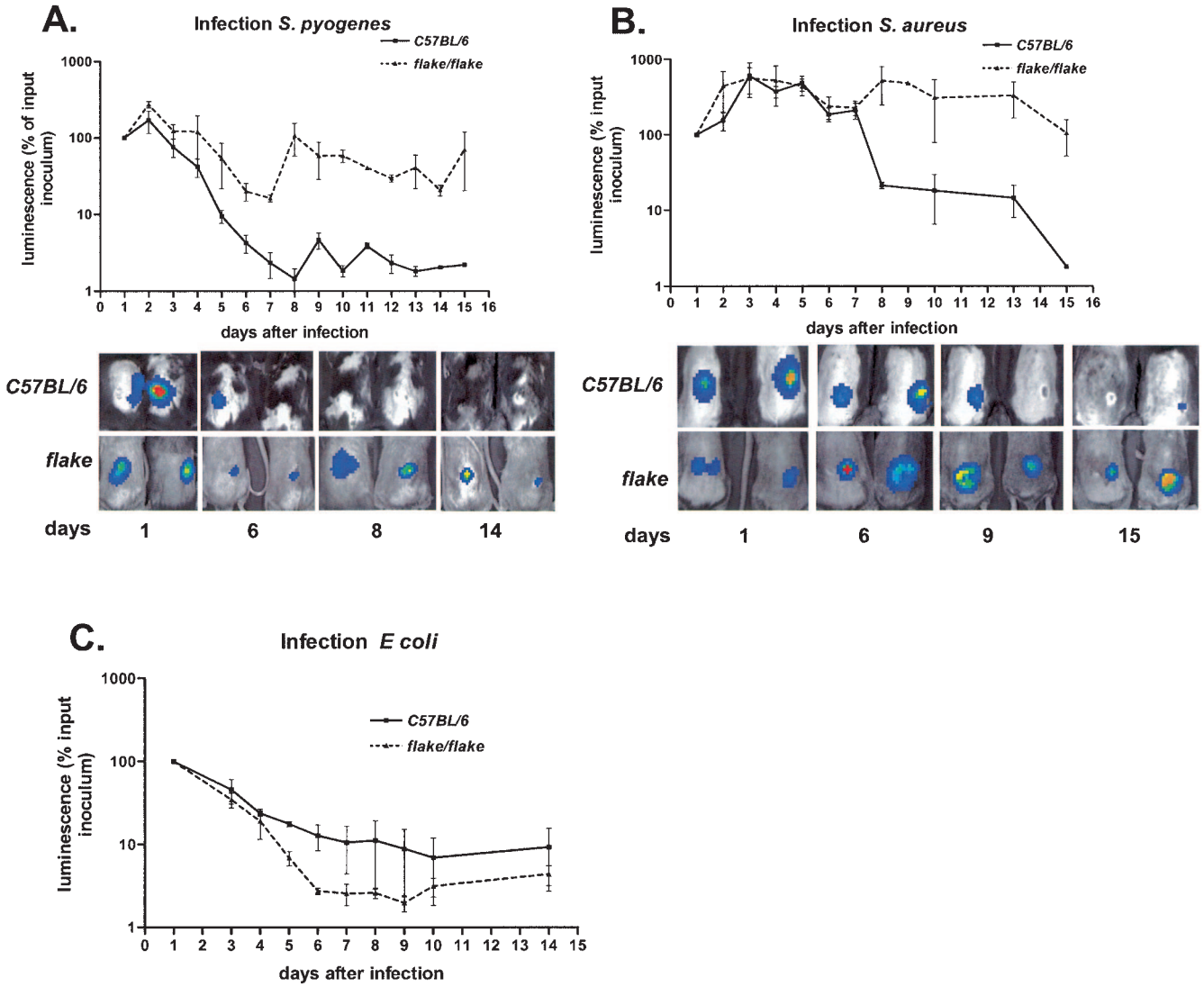


FIG. 2. *flake* mutant mice develop persistent skin infections when exposed to gram-positive bacteria. (A and B) Time course analyses of the bacterial growth in control (C57BL/6) ($n = 4$) and mutant (*flake*/*flake*) ($n = 4$) animals subcutaneously infected with *S. pyogenes* (A) or *S. aureus* (B). (Upper panels) Graphs show results of quantification by luminescence (expressed as a percentage of the luminescence in the initial inoculum) for four animals of each genotype. (Lower panels) Overlay of photographs and light detection for two representative mice for each genotype at the indicated days after inoculation. (C) Infection with *E. coli*.

C57BL/6 mice needed 8 days to completely clear a skin infection established by inoculation of $5 \times 10^5$ CFU of *S. pyogenes*. The *flk*/*flk* mutants showed similar kinetics of microbial clearance for the first 6 days following inoculation, but thereafter, the microbial burden in *flk*/*flk* mutants departed from control values, rising to reach a plateau that was maintained throughout the duration of the experiment. Luminescence slowly declined to reach background levels 4 weeks after inoculation in *flk*/*flk* mutants (not shown).

*S. pyogenes* produces a small, ulcerated wound, which healed almost completely by day 8 in control mice. Ulceration was still observed in *flk*/*flk* mutant mice up to 28 days after infection, albeit without detectable luminescence in vivo. Luminescent *S. pyogenes* bacteria were recovered by culturing the ulcers of *flk*/*flk* mutants. Hence, even 4 weeks after experimental inoculation, *flk*/*flk* mutant mice remained persistently infected with *S. pyogenes*.

Infection with *S. aureus* (Fig. 2B) yielded results formally similar to those described above. During the initial period of observation, the bacterial burden in *flk*/*flk* mutants closely matched that in controls, but a departure in the two curves was observed on day 7 following inoculation, with gradual clearance achieved in control animals (but not in *flk*/*flk* mutants), leading to a complete recovery of the controls within 2 weeks. In contrast, luminescence remained strongly detectable in *flake* mice for more than 3 weeks and reached background levels later than 4 weeks after inoculation (not shown).

On the other hand, *flk*/*flk* mutants were able to clear an infection with the gram-negative bacterium *Escherichia coli* (Fig. 2C). Moreover, no difference between *flk*/*flk* mutants and

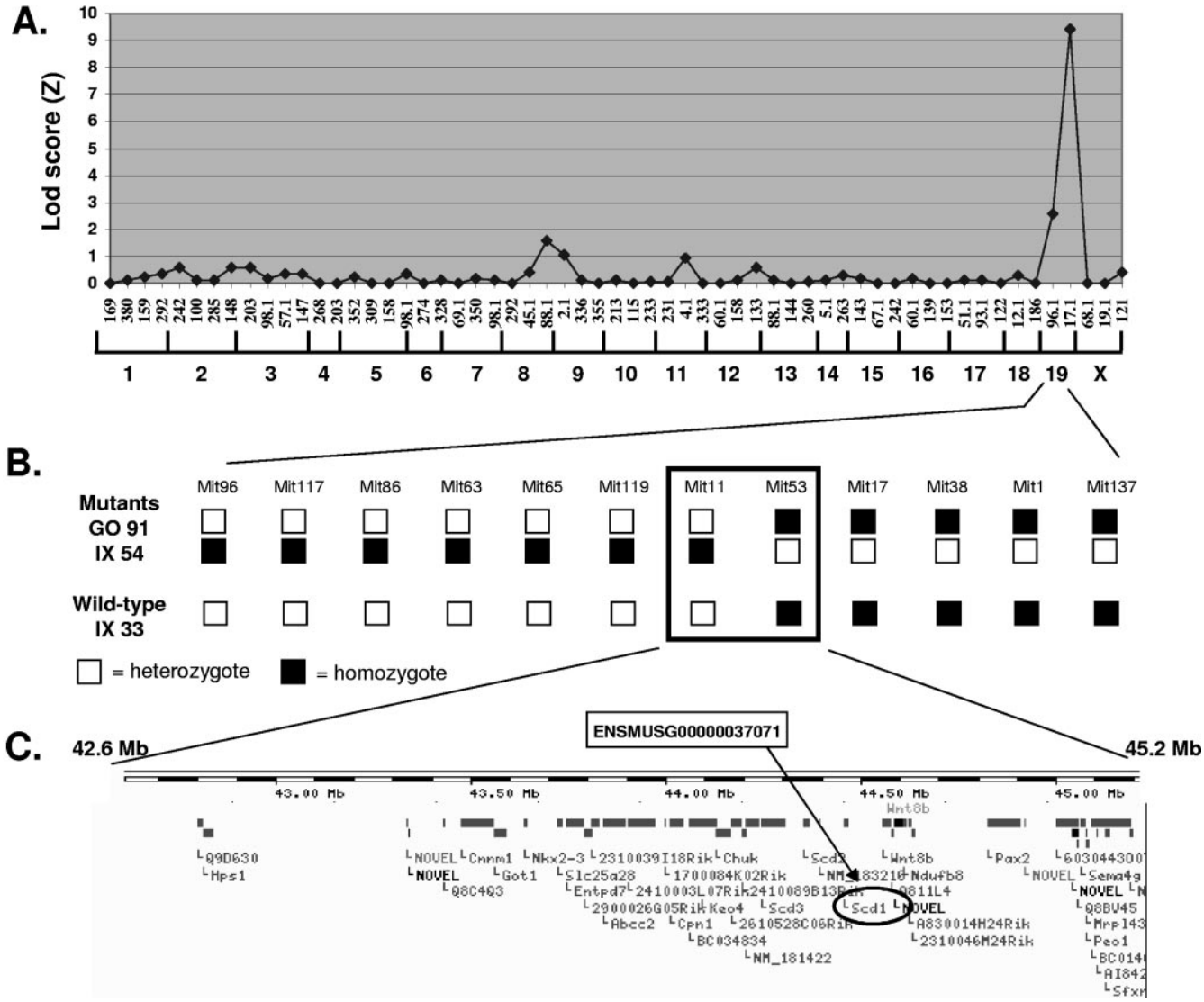


FIG. 3. Mapping of the *flake* mutation. (A) Transgenomic log likelihood ratio [Lod score (Z)] analysis shows a single peak of linkage on mouse chromosome 19. A total of 59 informative markers (horizontal axis) were included in the analysis, and 39 meioses (19 wild-type and 17 mutant animals) were genotyped at all markers. (B) Fine mapping of the distal region of chromosome 19. Analysis of a total of 283 meioses (3 representatives are shown) led to the confinement of the *flake* mutation between two adjacent markers 2.6 Mb apart. (C) Gene organization at the *flake* locus according to the Ensembl database. The *Scd1* gene is circled.

normal controls was observed when infections with gram-positive bacteria were introduced by other routes (for example, by intravenous inoculation of *Listeria monocytogenes* or by intrapulmonary challenge using *S. aureus* [not shown]). On the basis of all the data adduced in these studies, it appears that (i) *flk*/*flk* mutants mice are impaired in their ability to sterilize skin infections with gram-positive bacteria; (ii) the phenotype does not extend to all biological compartments and, so far as we know, is limited to the skin; (iii) the single infection with a gram-negative bacterium that was examined was not affected by the mutation; and (iv) the fact that skin lesions induced by *E. coli* healed normally in *flk*/*flk* mice indicates that the mutation does not affect wound healing per se but rather has a selective effect on pathogen clearance.

**Mapping of the *flk* mutation to the stearoyl CoA desaturase 1 locus.** The visible phenotype imparted by *flk* was utilized in mapping, and concordance between visible and immunologic phenotypes was later established by examining the progeny of intercrossed $F_1$ mice as well as other allelic variants of the locus (not shown). *flk* was initially mapped to chromosome 19 on 39 meioses by using a panel of 59 informative markers distributed throughout the mouse genome, in a backcross against C3H/HeN. The phenotype was fully penetrant on the mixed background, and the mutation was placed between markers D19Mit96 and D19Mit17 (Fig. 3A). Fine mapping was then performed using 12 internal chromosome-19 markers, so that on 283 meioses, the mutation was restricted to a 2.6-Mbp critical region delimited by D19Mit11 and D19Mit53 (Fig. 3B).

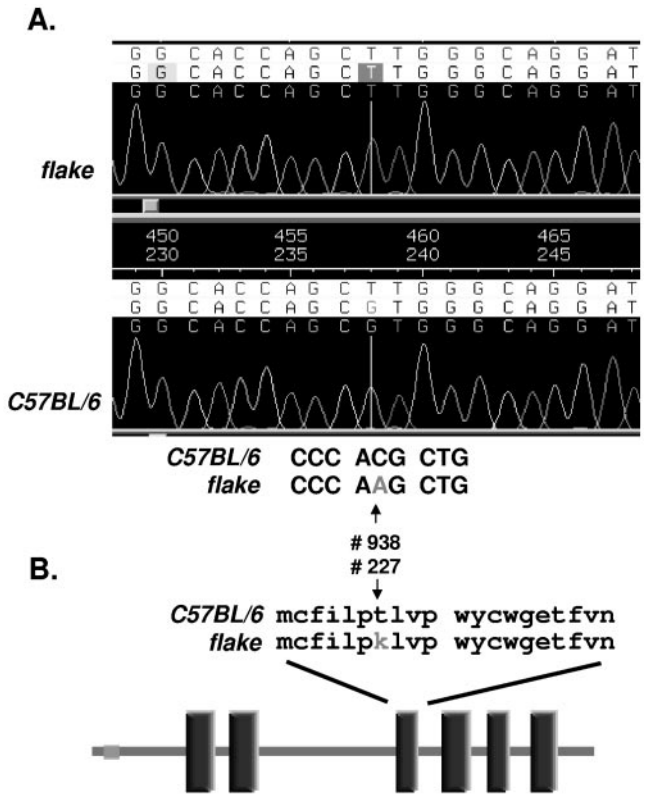


FIG. 4. Molecular characterization of the *flake* mutation. (A) Trace file of amplified genomic DNA from homozygous *flake* mutant mice (top chromatogram) and normal animals (bottom chromatogram). (B) Schematic representation of the SCD1 protein and localization of the *flake* mutation. Vertical rectangles correspond to transmembrane domains predicted by SMART analysis.

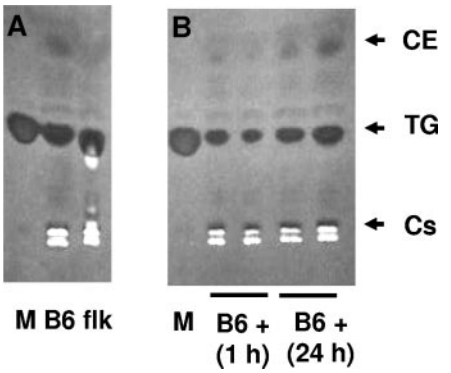


FIG. 5. TLC analysis of the lipid content in wild-type and *flake* mutant mice. (A) TLC of lipids extracted from skin biopsy specimens of wild-type (B6) or *flake* (flk) mutant mice. (B) TLC of lipids purified from the skin of wild-type mice (B6 +) 1 h or 24 h after *S. aureus* subcutaneous infection. Lanes M, markers. Cs, cholesterol; TG, triglycerides; CE, cholesterol esters.

Among the 43 genes represented within this region in the Ensembl database (Fig. 3C), we considered the stearyol coenzyme A (CoA) desaturase 1 (*Scd1*) gene a likely candidate, since two mutant alleles, named *asebia-J* and *asebia-2J*, have already been described for *Scd1* and in both cases, mutant mice show a cutaneous phenotype described as "scaly skin" (19, 29), similar to that observed in *flk* homozygotes.

The six exons of *Scd1* were amplified from genomic DNA isolated from both C57BL/6 control mice and *flk/flk* mutants. Direct sequencing of the amplicons revealed a point mutation (C to A) in exon 5, which corresponds to position 938 in the cDNA sequence (NCBI accession number BC055453) (Fig. 4A). This ENU-induced base transversion is predicted to cause a missense mutation (T227K) within SCD1. No mutation was detected in *Scd2* and *Scd3* cDNAs.

The microsomal enzyme SCD1 is an iron-binding 41-kDa protein of 355 amino acids with six predicted transmembrane domains. It catalyzes Δ9 desaturation of long-chain unsaturated fatty acids, leading to the biosynthesis of palmitoleate ($C_{16:1}$) and oleate ($C_{18:1}$) as its major products. As shown in Fig. 4B, the substitution of a neutral amino acid (T) for a charged residue (K) in the mutated protein occurs within a predicted transmembrane domain and would be expected to disrupt the structural integrity of SCD1.

To test this assumption, we performed TLC to analyze the lipid composition of skin biopsy specimens from control and *flk/flk* mice. The latter animals exhibit a reduction in cholesterol esters (Fig. 5A), similar to that reported in the case of *Scd1* knockout (KO) mice, which indicates that the *flk* phenotype is indeed caused by the observed allelic variant of *Scd1*.

**Palmitoleate and oleate have intrinsic antibacterial activity in vitro and in vivo.** The absence of $C_{18}$ and $C_{16}$ fatty acid desaturase activity in $Scd1^{flk/flk}$ mutant mice prompted us to ask whether the lack of oleate and/or palmitoleate could account for the cutaneous immunodeficiency phenotype described above. Indeed, several reports have indicated that MUFA exhibit antimicrobial activity against gram-positive bacteria (12, 24), though there is no evidence that MUFA exert a protective effect in vivo. To test our working hypothesis, we first performed a series of in vitro experiments in which we measured the effect of each lipid on the growth of *S. pyogenes*, *S. aureus*, and *E. coli*.

Our results confirmed that palmitoleate and oleate each have strong bacteriostatic and bactericidal activities against *S. pyogenes* and *S. aureus*. The MICs (Table 1) of both compounds for *S. pyogenes* are in the micromolar range and com-

TABLE 1. MICs and minimum bactericidal concentrations of CRAMP, oleic acid, and palmitoleic acid for *S. pyogenes* and *S. aureus*

| Bacterium | MIC (μM) of: | | | MBC [a] (μM) of: | | |
|---|---|---|---|---|---|---|
| | CRAMP | Oleate | Palmitoleate | CRAMP | Oleate | Palmitoleate |
| *S. pyogenes* | 5.3 ± 2.3 | 8.3 ± 2.9 | 10 ± 0.1 | 11.3 ± 5.8 | 13.3 ± 5.8 | 10 ± 0.1 |
| *S. aureus* | Resistant | >75 | 36.6 ± 11.5 | Resistant | ND | 50 ± 15 |

[a] MBC, minimum bactericidal concentration; ND, not determined.

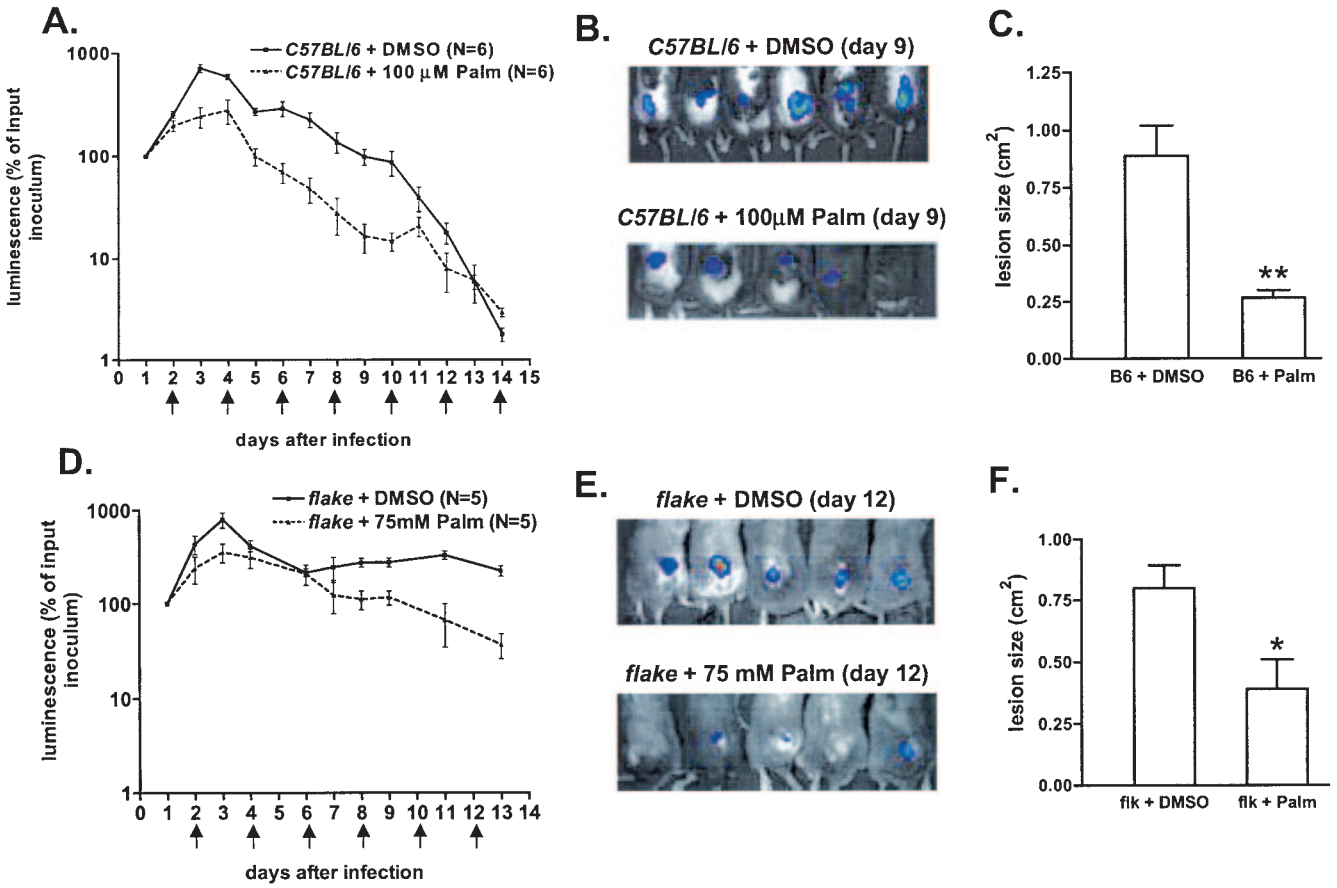


FIG. 6. Palmitoleic acid has antibacterial activity in vivo. (A) Palmitoleate (Palm) injection accelerates bacterial clearance in wild-type mice. Luminescence (expressed as a percentage of the luminescence in the initial inoculum) was measured in control (C57BL/6) mice inoculated with *S. aureus* (at day 0) and treated by vehicle (DMSO) or palmitoleate injections every 2 days (arrows). (B) Photographs, taken 9 days after *S. aureus* infection, of control (C57BL/6) mice treated by DMSO (top) or palmitoleate (bottom) injections. (C) Histogram showing the sizes of lesions measured at day 9 after infection in control (B6) mice treated with DMSO or palmitoleate. **, $P < 0.01$. (D) Palmitoleate treatment of *S. aureus*-infected *flake* mice. The protocol is similar to that for panel A, except that we performed 100-μl injections of a 75 mM solution of palmitoleate. (E) Photographs of infected *flake* mice at day 12 after DMSO (top) or palmitoleate (bottom) treatment. (F) Sizes of lesions (determined at day 12) in infected *flk* mutants treated with DMSO or palmitoleate. *, $P < 0.05$.

parable to that observed for the murine cathelicidin AMP (CRAMP). On a weight basis, the MUFA are therefore approximately 20 times as potent as cathelicidin. MUFA are also active against *S. aureus*, whereas CRAMP is totally inactive. On the other hand, no bacteriostatic or bactericidal activity was detected against *E. coli* even at millimolar MUFA concentrations (not shown), consistent with a specific effect against gram-positive bacteria.

To investigate the physiological relevance of this antimicrobial activity, we inoculated wild-type mice with *S. aureus* and treated the infected animals by repeated (every 2 days) subcutaneous injections of palmitoleate (100 μl of a 100 μM solution in dimethyl sulfoxide [DMSO]) or DMSO alone at the site of infection. The results of this experiment are shown in Fig. 6A and B. For both groups of mice ($n = 6$ animals), luminescence is expressed as a percentage of the luminescence of the initial inoculum, determined 24 h after infection. Nine days after *S. aureus* inoculation, palmitoleate-treated animals exhibited a 90% reduction in luminescence, compared to vehicle-treated mice. As a consequence of improved *S. aureus* elimination, the diameter of the ulcerative wound (measured at day 9) in lipid-treated animals was one-fourth that observed in controls (Fig. 6C). These data, which clearly illustrate the antibacterial capacities of MUFA in vitro and in vivo, also reveal that this lipid-based defense mechanism is not maximally efficacious in normal mice.

Under similar conditions of palmitoleate administration, *flake* mutants exhibited a marked reduction in bacterial growth between days 1 and 4 (also observed in wild-type mice), but *S. aureus* remained detectable 2 weeks after inoculation (not shown). As shown in Fig. 6D and E, a higher dose of palmitoleate (100 μl of a 75 mM solution) moderately improved bacterial clearance in *flk/flk* mutants and the subsequent ulcer healing (Fig. 6F). However, complete rescue of the phenotype was not achieved by this pharmacological approach (see Discussion).

**Transcriptional activation of *Scd1* occurs during gram-positive bacterial infection and is TLR2 dependent.** The unsuspected in vivo antimicrobial function of MUFA prompted us to ask whether their synthesis is increased during the immune

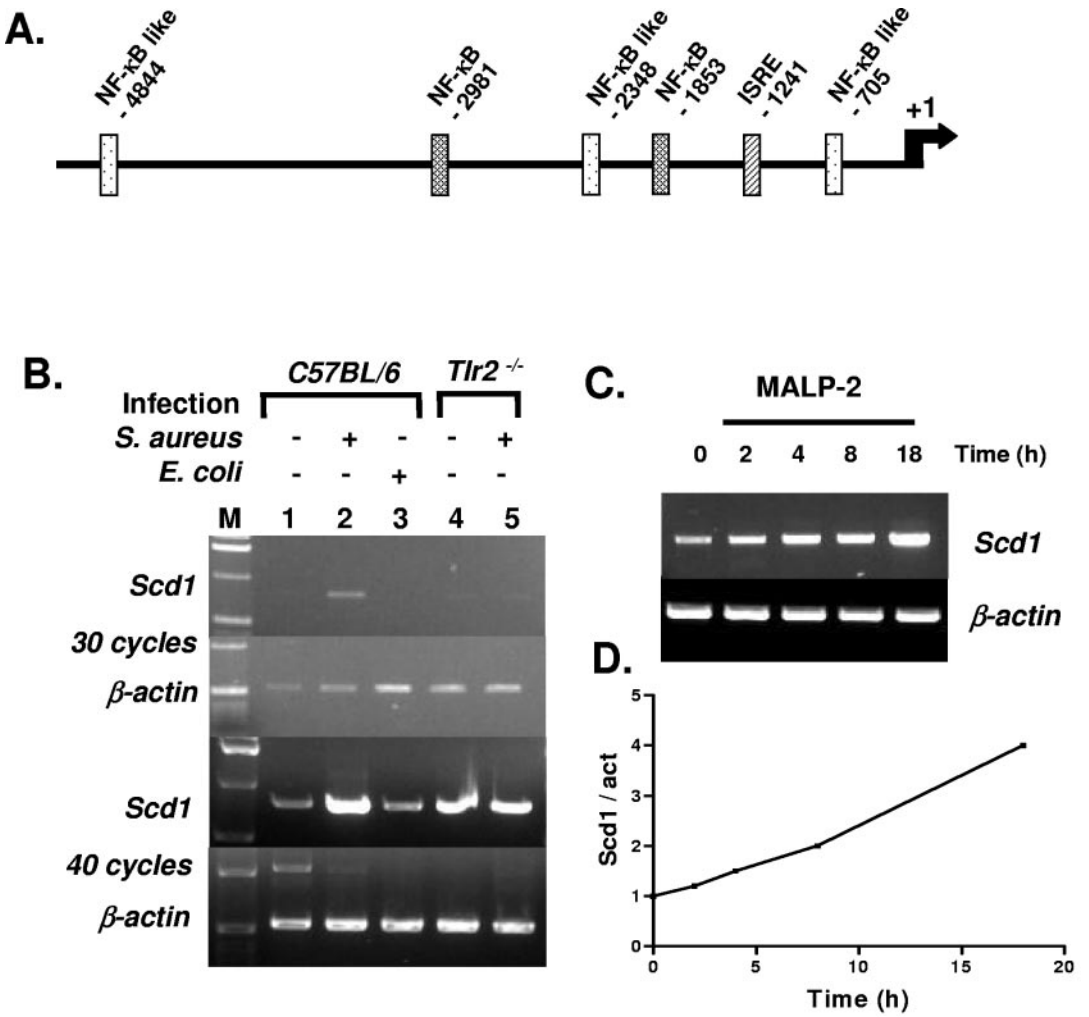


FIG. 7. Infection- and TLR2-dependent induction of *Scd1* gene expression in mice. (A) SignalScan analysis of the *Scd1* promoter. NF-κB and ISRE (interferon-stimulated regulatory element) are shown. (B) RT-PCR detection of *Scd1* and β-*actin* transcripts in skin biopsy specimens of uninfected control (C57BL/6) and *Tlr2*$^{-/-}$ animals (lanes 1 and 4) or after infection by *S. aureus* (lanes 2 and 5) or *E. coli* (lane 3). PCR products obtained after 30 and 40 cycles are shown. M, size standard. (C) RT-PCR detection of *Scd1* and β-*actin* transcripts in control (0 h) and MALP-induced peritoneal macrophages isolated from wild-type mice after 2, 4, 8, and 18 h. (D) Quantification of the Scd1/β-actin ratio.

response, as is the case for other effector molecules such as CRAMP. We analyzed a 5-kb fragment of the *Scd1* promoter and noted the presence of several NF-κB binding sites (Fig. 7A). We then performed semiquantitative RT-PCR experiments on skin biopsy specimens from normal or infected mice. Figure 7B shows that *Scd1* mRNA accumulation is strongly induced in the skin of control (C57BL/6) mice upon *S. aureus* infection, whereas *E. coli* inoculation produces no effect. Furthermore, in mice carrying a targeted disruption of the *Tlr2* gene (*Tlr2*$^{-/-}$), the *Scd1* gene is unresponsive to inoculation of gram-positive bacteria. However, *Scd1* transcriptional induction might also be caused by an indirect mechanism, given the 24-h delay between infection and RNA isolation.

Macrophages, which represent an ideal system in which to study TLR signaling, also express the *Scd1* gene, as reported recently (22). To determine whether isolated macrophages are capable of up-regulating *Scd1* and to determine the kinetics of the response, we stimulated peritoneal macrophages isolated from wild-type mice with synthetic MALP-2 (EMC microcollections GmbH, Tübingen, Germany), a known TLR2 agonist (21). We surveyed *Scd1* expression by RT-PCR on RNA samples isolated 2, 4, 8, and 18 h after stimulation. As seen in Fig. 7C and D, *Scd1* expression was augmented 2 h after MALP induction and reached a fourfold increase within 18 h. This transcriptional induction of *Scd1* was correlated with increased lipid synthesis in the skin of infected animals (Fig. 5B).

As previously noted, *Scd1* is expressed principally in sebaceous glands, and *flake* mice, as well as *asebia* and *Scd1* KO mice, exhibit atrophy of these structures (not shown). To corroborate the potential relevance of inducible *Scd1* expression in human skin defense against gram-positive pathogens, we investigated the effect of MALP-2 on the immortalized human sebocyte cell line SZ95 (30). First, we noted that treatment with MALP-2, but not with LPS, induced a rapid and potent inflammatory response, manifested by increased IL-6 and IL-8 production (Fig. 8A and B). Next, we observed that *SCD1*

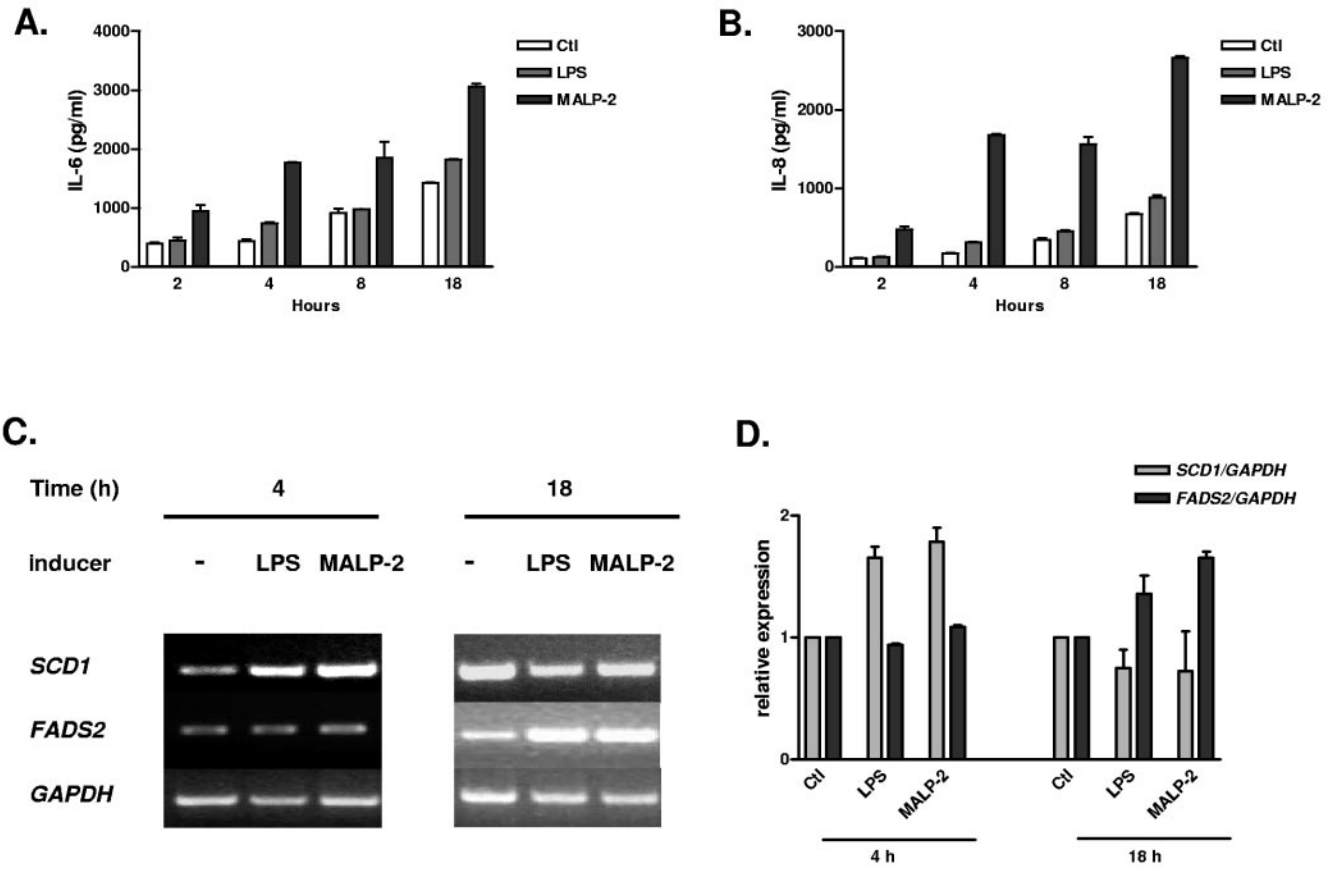


FIG. 8. Human sebocytes stimulated with MALP-2 show an inflammatory response and up-regulation of *SCD1* and *FADS2* genes. (A) IL-6 production is induced in SZ95 cells after MALP-2 treatment (50 ng/ml). LPS stimulation (100 ng/ml) shows minimal effect. (B) Quantification of IL-8 under the same conditions as those in panel A. (C) RT-PCR detection of *SCD1* and *FADS2* expression 4 and 18 h after LPS and MALP-2 stimulation. GAPDH expression was used as a control. (D) Quantification of the *SCD1* and *FADS2* signals measured in two independent experiments (± standard errors of the means) after normalization with the *GAPDH* signal.

transcription is also up-regulated in this human cell line 4 h after MALP-2 stimulation (Fig. 8C and D). We extended these observations by monitoring the expression of the fatty acid desaturase 2 (*FADS2*) gene. *FADS2* encodes a protein with enzymatic properties similar to those of SCD1 and was recently shown to be deficient in a patient affected by a severe skin condition (25) manifested by cheilosis, a hyperkeratotic rash over the arms and legs, and perineal dermatitis. In human cultured sebocytes, *FADS2* is slightly but specifically induced 18 h after MALP-2 stimulation.

## DISCUSSION

SCD1 is an enzyme responsible for the biosynthesis of MUFA, mainly palmitoleate ($C_{16:1}$) and oleate ($C_{18:1}$) (15). It catalyzes Δ9 *cis*-desaturation of the carbon chain and uses palmitoyl-CoA and stearoyl-CoA as substrates. The functions of this enzyme in lipid metabolism have been intensely studied (16). *Scd1*$^{-/-}$ mice are significantly leaner than wild-type animals and are resistant to diet-induced adiposity, an effect mediated by increased expression of genes involved in fatty acid oxidation. Furthermore, compound homozygotes for hypomorphic mutations of the *obese* (*ob*) and *Scd1* genes exhibit a striking attenuation of the *obese* phenotype (17). The observation that *Scd1* is overexpressed in *ob* mutants indicates that at least part of the leptin's metabolic actions result from the inhibition of *Scd1* (3). Two spontaneous mutant alleles of *Scd1* have been described and named *asebia-J* (*ab-J*) and *ab-2J* (19, 29). Despite minor phenotypic differences, homozygosity for each of these alleles is associated with atrophic sebaceous glands, alopecia, and scaly skin, phenotypes which are also observed in mice carrying a targeted disruption of the gene (13).

In the present study, we have described *flake*, a visible recessive phenovariant with a highly selective innate immunodeficiency phenotype, in which there is failure to eliminate gram-positive (but not gram-negative) organisms from the skin. Using a phenotype-driven approach, we tracked the *flk* mutation to a missense error (T227K) that falls within the fourth of six transmembrane domains of the SCD1 protein. The replacement of a neutral by a charged residue in such a region might alternatively modify the conformation of the desaturase, which normally resides within microsomal membranes, or affect coordination of the iron atom that is necessary for enzymatic activity. Whatever the mechanism, we have demonstrated a reduction in the level of cholesterol esters (the biosynthesis of

which requires MUFA) in lipid isolates from the skin of *flake* mutant mice, confirming that the new allele is hypofunctional.

Here we have implicated SCD1 and the products of its catalytic activity in epithelial innate immunity against gram-positive bacteria. It has been shown previously that feeding *Scd1*-deficient mice a MUFA-enriched diet does not alleviate the mutant phenotype, which indicates that de novo synthesis of MUFA is required for normal appearance and function of the skin. Therefore, to extend our in vitro observations, we monitored the effect of intradermal administration of palmitoleate to *S. aureus*-infected mice. These in vivo experiments showed that repeated subcutaneous injections of palmitoleate reduced bacterial proliferation and significantly improved the recovery of infected mice, as evidenced by reduction of the ulcerative wound. However, this beneficial effect of palmitoleic acid was less pronounced in *flake* mutants, despite repeated injections of higher doses of palmitoleate. The complex lipidic composition of the sebum, whose overall production is reduced in *flake* mutant animals, might account for this observation. It is, therefore, conceivable that antibacterial lipids (12) other than MUFA may be required for efficient clearance of the infection. Alternatively, the overactivated lipid catabolism observed in *Scd1* mutants might lead to a shorter half-life of the injected lipids and could explain this discrepancy. Nevertheless, we noted that humans treated for acne problems with retinoids (which induce atrophy of the sebaceous glands) can suffer recurrent *S. aureus* skin infections as a side effect (10). Infections of the eye with gram-positive bacteria have also been noted in such patients (4). Indeed, we have also observed eye infections in *flake* mutants (Fig. 1C), as noted previously for *Scd1* KO mice (13). Our data from *flk*/*flk* mice emphasize the essential role of sebaceous glands, as well as other lipid-producing organs, including perhaps the specialized meibomian glands of the eyelids, in local innate immune responses.

The mechanism by which MUFA selectively kill gram-positive bacteria remains to be determined. The length of the carbon chain and/or the level of unsaturation might be important determinants of efficacy. In addition, synergy between lipids and AMP might also be examined. *flake*/*CRAMP* double-knockout mice will prove to be useful tools with which to study this issue. Our experiments do not exclude the possibility that, in addition to their antimicrobial activity, palmitoleate and oleate might promote resistance indirectly. Modulation of signal transduction through protein modification might be one such mechanism. As reported elsewhere (11), mass spectrometry identified palmitoleate among other posttranslational modifications of the src homology domain 3 kinase Fyn, which might affect immune cell activation, as recently shown for insulin signaling in muscle cells (18).

*SCD1* transcription is strongly up-regulated in mouse and human cells in a TLR2-dependent manner. Human patients with rare skin disorders such as the syndrome of ichthyosis follicularis with atrichia and photophobia (IFAP syndrome; OMIM 308205) possess atrophic sebaceous glands and coincidently suffer alopecia and recurrent skin infections reminiscent of the *Flake* phenotype (reviewed in reference 1). With new recognition that TLR2 and -6 are expressed in human sebocytes (C. C. Zouboulis et al., unpublished data), our results point to a prominent and unsuspected role of the sebaceous gland in the innate immune defense of the skin. Altogether, our data demonstrate the existence of an inducible lipid-based microbicidal effector pathway in the skin and establish a clear functional link between lipid metabolism and innate immunity.

## ACKNOWLEDGMENTS

This work was supported by a grant from the NIH (U54 A154523), the Fondation Philippe (to P.G.), and the Verein zur Förderung der Dermatologie (to C.C.Z.).

## REFERENCES

1. **Alfadley, A., H. K. Al, and A. K. Al.** 2003. Ichthyosis follicularis: a case report and review of the literature. Pediatr. Dermatol. **20:**48–51.
2. **Bunce, C., L. Wheeler, G. Reed, J. Musser, and N. Barg.** 1992. Murine model of cutaneous infection with gram-positive cocci. Infect. Immun. **60:**2636–2640.
3. **Cohen, P., M. Miyazaki, N. D. Socci, A. Hagge-Greenberg, W. Liedtke, A. A. Soukas, R. Sharma, L. C. Hudgins, J. M. Ntambi, and J. M. Friedman.** 2002. Role for stearoyl-CoA desaturase-1 in leptin-mediated weight loss. Science **297:**240–243.
4. **Egger, S. F., V. Huber-Spitzy, K. Bohler, and C. Scholda.** 1995. Isotretinoin administration in treatment of acne vulgaris. A prospective study of the kind and extent of ocular complications. Ophthalmologe **92:**17–20. (In German.)
5. **Guay, D. R.** 2003. Treatment of bacterial skin and skin structure infections. Expert Opin. Pharmacother. **4:**1259–1275.
6. **Hedrick, J.** 2003. Acute bacterial skin infections in pediatric medicine: current issues in presentation and treatment. Paediatr. Drugs **5**(Suppl. 1)**:**35–46.
7. **Hoebe, K., X. Du, J. Goode, N. Mann, and B. Beutler.** 2003. Lps2: a new locus required for responses to lipopolysaccharide, revealed by germline mutagenesis and phenotypic screening. J. Endotoxin Res. **9:**250–255.
8. **Kraft, W. G., P. T. Johnson, B. C. David, and D. R. Morgan.** 1986. Cutaneous infection in normal and immunocompromised mice. Infect. Immun. **52:**707–713.
9. **Kuklin, N. A., G. D. Pancari, T. W. Tobery, L. Cope, J. Jackson, C. Gill, K. Overbye, K. P. Francis, J. Yu, D. Montgomery, A. S. Anderson, W. McClements, and K. U. Jansen.** 2003. Real-time monitoring of bacterial infection in vivo: development of bioluminescent staphylococcal foreign-body and deep-thigh-wound mouse infection models. Antimicrob. Agents Chemother. **47:**2740–2748.
10. **Leyden, J. J., K. J. McGinley, and A. N. Foglia.** 1986. Qualitative and quantitative changes in cutaneous bacteria associated with systemic isotretinoin therapy for acne conglobata. J. Investig. Dermatol. **86:**390–393.
11. **Liang, X., Y. Lu, M. Wilkes, T. A. Neubert, and M. D. Resh.** 2004. The N-terminal SH4 region of the Src family kinase Fyn is modified by methylation and heterogeneous fatty acylation: role in membrane targeting, cell adhesion, and spreading. J. Biol. Chem. **279:**8133–8139.
12. **Miller, S. J., R. Aly, H. R. Shinefeld, and P. M. Elias.** 1988. In vitro and in vivo antistaphylococcal activity of human stratum corneum lipids. Arch. Dermatol. **124:**209–215.
13. **Miyazaki, M., W. C. Man, and J. M. Ntambi.** 2001. Targeted disruption of stearoyl-CoA desaturase1 gene in mice causes atrophy of sebaceous and meibomian glands and depletion of wax esters in the eyelid. J. Nutr. **131:**2260–2268.
14. **Nizet, V., T. Ohtake, X. Lauth, J. Trowbridge, J. Rudisill, R. A. Dorschner, V. Pestonjamasp, J. Piraino, K. Huttner, and R. L. Gallo.** 2001. Innate antimicrobial peptide protects the skin from invasive bacterial infection. Nature **414:**454–457.
15. **Ntambi, J. M.** 1995. The regulation of stearoyl-CoA desaturase (SCD). Prog. Lipid Res. **34:**139–150.
16. **Ntambi, J. M., and M. Miyazaki.** 2004. Regulation of stearoyl-CoA desaturases and role in metabolism. Prog. Lipid Res. **43:**91–104.
17. **Ntambi, J. M., M. Miyazaki, J. P. Stoehr, H. Lan, C. M. Kendziorski, B. S. Yandell, Y. Song, P. Cohen, J. M. Friedman, and A. D. Attie.** 2002. Loss of stearoyl-CoA desaturase-1 function protects mice against adiposity. Proc. Natl. Acad. Sci. USA **99:**11482–11486.
18. **Rahman, S. M., A. Dobrzyn, P. Dobrzyn, S. H. Lee, M. Miyazaki, and J. M. Ntambi.** 2003. Stearoyl-CoA desaturase 1 deficiency elevates insulin-signaling components and down-regulates protein-tyrosine phosphatase 1B in muscle. Proc. Natl. Acad. Sci. USA **100:**11110–11115.
19. **Sundberg, J. P., D. Boggess, B. A. Sundberg, K. Eilertsen, S. Parimoo, M. Filippi, and K. Stenn.** 2000. Asebia-2J ($Scd1^{ab2J}$): a new allele and a model for scarring alopecia. Am. J. Pathol. **156:**2067–2075.
20. **Takeda, K., and S. Akira.** 2003. Toll receptors and pathogen resistance. Cell. Microbiol. **5:**143–153.
21. **Takeuchi, O., A. Kaufmann, K. Grote, T. Kawai, K. Hoshino, M. Morr, P. F. Muhlradt, and S. Akira.** 2000. Preferentially the R-stereoisomer of the mycoplasmal lipopeptide macrophage-activating lipopeptide-2 activates immune cells through a toll-like receptor 2- and MyD88-dependent signaling pathway. J. Immunol. **164:**554–557.

22. **Uryu, S., S. Tokuhiro, and T. Oda.** 2003. β-Amyloid-specific upregulation of stearoyl coenzyme A desaturase-1 in macrophages. Biochem. Biophys. Res. Commun. **303:**302–305.
23. **Vidal, F., D. Aberdam, C. Miquel, A. M. Christiano, L. Pulkkinen, J. Uitto, J. P. Ortonne, and G. Meneguzzi.** 1995. Integrin beta 4 mutations associated with junctional epidermolysis bullosa with pyloric atresia. Nat. Genet. **10:** 229–234.
24. **Wille, J. J., and A. Kydonieus.** 2003. Palmitoleic acid isomer ($C_{16:1}\Delta6$) in human skin sebum is effective against gram-positive bacteria. Skin Pharmacol. Appl. Skin Physiol. **16:**176–187.
25. **Williard, D. E., J. O. Nwankwo, T. L. Kaduce, S. D. Harmon, M. Irons, H. W. Moser, G. V. Raymond, and A. A. Spector.** 2001. Identification of a fatty acid Δ6-desaturase deficiency in human skin fibroblasts. J. Lipid Res. **42:**501–508.
26. **Witkop, C. J., Jr., J. G. White, R. A. King, M. V. Dahl, W. G. Young, and J. J. Sauk, Jr.** 1979. Hereditary mucoepithelial dysplasia: a disease apparently of desmosome and gap junction formation. Am. J. Hum. Genet. **31:**414–427.
27. **Zasloff, M.** 2002. Antimicrobial peptides of multicellular organisms. Nature **415:**389–395.
28. **Zasloff, M.** 2002. Antimicrobial peptides in health and disease. N. Engl. J. Med. **347:**1199–1200.
29. **Zheng, Y., K. J. Eilertsen, L. Ge, L. Zhang, J. P. Sundberg, S. M. Prouty, K. S. Stenn, and S. Parimoo.** 1999. Scd1 is expressed in sebaceous glands and is disrupted in the asebia mouse. Nat. Genet. **23:**268–270.
30. **Zouboulis, C. C., H. Seltmann, H. Neitzel, and C. E. Orfanos.** 1999. Establishment and characterization of an immortalized human sebaceous gland cell line (SZ95). J. Investig. Dermatol. **113:**1011–1020.

*Editor:* F. C. Fang